

LUMEN DETECTION IN IVUS IMAGES USING SNAKES IN A STATISTICAL FRAMEWORK

Oriol Pujol, Petia Radeva

Centre de Visió per Computador
Universitat Autònoma de Barcelona
Edifici O, Campus UAB.

ABSTRACT

Intravascular Ultrasound Images (IVUS) are an excellent tool for direct visualization of vascular pathologies and evaluation of the lumen and plaque in coronary arteries. Nowadays, the most common methods to separate the tissue from the lumen are based on gray levels providing non-satisfactory segmentations. In this paper we propose a new deformable model defined in a statistic framework to segment IVUS images. We perform a supervised learning of local texture patterns of the plaque region and construct a feature space using a set of co-occurrence matrix measures. Linear Discriminant Analysis allows to obtain an optimal reduced feature space where a gaussian mixture model is applied to construct a likelihood map. Instead of using heuristic potential field, we propose the usage of a regularized version of the likelihood map in order to segment the lumen. The snake deforms on the likelihood map until it captures likelihood contours. Different tests on medical images show the advantages of our statistic deformable model.

1. INTRODUCTION

Intravascular Ultrasound Images (IVUS) is a relatively new technique that offers image information data of cross-sectional cuts of the vessel. Therefore, it facilitates analysis of atherosclerotic plaque composition, allowing to distinguish among lumen, plaque and vessel wall, as well as the composition of some of the tissues. Growing evidence exists suggesting that the structure and composition of atherosclerotic plaque play important roles in coronary artery disease and in the outcomes of coronary interventions. However, visual evaluation and characterization of plaque require integration of complex information and suffer from substantial variability depending on the observer. This fact explains the difficulties of manual segmentation prone to high subjectivity in final results. Automatic segmentation will save time to physicians and provide objective vessel measurements.

The problem of texture analysis has played a prominent role in computer vision to solve problems of object

segmentation and retrieval in numerous applications.[1] [2] Two approaches are used for texture analysis, supervised and unsupervised analysis. However, an important problem in both approaches is precise location of textured object boundaries. This is due to the low likelihood of the texture boundaries to belong to learned texture regions. Therefore, changes in the likelihood map provides good candidate locations to find texture boundaries.

Previous works has shown different ways to segment lumen [3] [4] [5] [6] [7]. However, most of them suffers from misclassifications due to the appearance of artifacts (the guide effect, the catheter effect and other structures due to deficiencies in the acquisition) or propose semi-automatic segmentations. In our work we show an automatic segmentation method able to deal with artifacts making their influence almost negligible.

The objective of our work is to provide a statistic approach for IVUS segmentation framework using statistic deformable models. The main contribution of our work is threefold: a) we propose a segmentation method for reliable plaque detection, b) we propose an improved active contour model that deforms on a likelihood map instead of heuristically constructed edge map.

2. METHODOLOGY OF IVUS TEXTURE ANALYSIS BY STATISTIC DEFORMABLE MODELS

2.1. Texture analysis

The Gray Level Co-occurrence Matrix is a well-known statistical tool for extracting second-order texture information from images [8]. In the co-occurrence method, the relative frequencies of gray level pairs of pixels at certain relative displacement are computed and sorted in a matrix, the *co-occurrence matrix* \mathbf{P} . For G gray levels in the image, \mathbf{P} will be of size $G \times G$. The element values in the matrix, when normalized are bounded by $[0, 1]$, and the sum of all element values is equal to 1. The co-occurrence matrix is defined by $P(i, j, D, \theta) = (P(I(l, m) = i \text{ and } I(l + D \cos(\theta), m + D \sin(\theta)) = j)$ where $I(l, m)$ is the image at pixel (l, m) , D is the distance between pixels and θ is the angle. It has been proved by other researchers [9] [10] that the nearest neighbor pairs at distance D at ori-

This work was partially supported by the project TIC2000-1635-CO4-04 of CICYT, Ministerio de Ciencia y Tecnología of Spain.

entations $\theta = \{0^\circ, 45^\circ, 90^\circ, 135^\circ\}$ are the minimum set needed to describe the texture second-order statistic measures. Once the co-occurrence matrix is computed, features must be extracted. The features used for our study are Energy, Entropy, Inverse Difference Moment (IDM), Shade, Inertia and Promenace. Hence, given four different orientations and the six measures in each orientation, our feature vector will be a 24 dimensional vector for each pixel.

2.2. Feature data dimensionality reduction and texture modeling

The feature vector is composed of redundant data so a *dimensional reduction* can be considered as a previous step to the texture modeling. A classical approach to find effective linear transformation is the discriminant analysis, which seeks directions that are efficient for discrimination. Therefore, we have used **Fisher Linear Discriminant Analysis** (FLDA) [11] for data dimensionality reduction. FLDA ensures a dimensionality reduction maximizing the discrimination among the classes. FLDA seeks a transformation matrix W such that the ratio of the between-class scatter $S_B = \sum_{i=1}^c N_i(\mu_i - \mu)(\mu_i - \mu)^T$ and the within-class scatter $S_W = \sum_{i=1}^c \sum_{x_{k,i} \in X_i} (x_{k,i} - \mu_i)(x_{k,i} - \mu_i)^T$ is maximized. where μ_i is the mean value of class X_i , μ is the mean value of the whole data, c is the number of classes and N_i is the number of samples in class X_i . If S_W is not singular, the optimal projection matrix W_{opt} is chosen as the matrix which maximizes the ratio of the determinant of the between-class scatter matrix of the projected samples to the determinant of the within-class scatter matrix of the projected samples:

$$W_{opt} = \underset{W}{\operatorname{argmax}} \frac{|W^T S_B W|}{|W^T S_W W|} = [\mathbf{w}_1, \mathbf{w}_2, \dots, \mathbf{w}_m] \quad (1)$$

where $\mathbf{w}_i, i = 1 \dots m$ is the set of S_W -generalized eigenvectors of S_B corresponding to the m largest generalized eigenvalues.

We assume that the projected data in the reduced space can be modeled using low-level statistics where their behaviors are expressed with conditional probability density functions which can be modeled using a Gaussian Mixture Model [11]. The mixture model is composed of a sum of fundamental distributions, following the next equation

$$p_i(x|\Theta) = \sum_{k=1}^C p_k(x|\theta_k) P_k \quad (2)$$

where C is the number of mixture components, P_k is the *a priori* probability of the component k and θ_k represents the unknown mixture parameters. In our case, we have chosen **gaussian mixture models** $\theta_k = \{P_k, \mu_k, \sigma_k\}$ for the plaque texture set.

2.3. Likelihood map interpretation by statistic snakes

The texture modeling process is the previous step for the likelihood map computation. The likelihood map measures how likely each of the pixels of the image is to belong to the desired pattern. It, also, allows us to define a higher-level approach based on deformable models, which will deal with the artifacts making their effect negligible.

2.3.1. Background of snakes

The basic target of active contours [12] is to find a parameterized curve that minimizes the weighted sum of its internal energy and external energy. Given a traditional snake curve $\mathbf{x}(s) = (x(s), y(s)), s \in [0, 1]$, the snake can be formulated as the minimization of the following equation:

$$S(\mathbf{x}) = \int_0^1 (\alpha(s)|\mathbf{x}'(s)|^2 + \beta|\mathbf{x}''(s)| + E_e) ds \quad (3)$$

The internal energy specifies the tension and smoothness of the contour. The external energy is derived from the image data. Regardless the external function the problem of finding the curve $\mathbf{x}(s)$ that balances the internal and external forces must satisfy the Euler-Lagrange equation which can be solved iteratively as follows:

$$\mathbf{x}_t(s, t) = \alpha \mathbf{x}''(s, t) - \beta \mathbf{x}''''(s, t) - \nabla E_e \quad (4)$$

The classic approach to the external energy is the potential energy which takes smaller values at object boundaries as well as other features of interest. The typical potential function designed to lead a deformable contour toward step edges is a function of the high-gradient location of the pixels of the original image $-|\nabla(G_\sigma(x, y) * I(x, y))|^2$ where $G_\sigma(x, y)$ is the gaussian filter of standard deviation σ , and $I(x, y)$ is the image data. As can be observed greater σ will increase the attraction range but the edges will blur.

Different convergence problems affect the performance of snakes: first a close initialization is usually needed, problems with stopping criterion, impossibility to converge to concave boundaries, etc. One of the most spread approaches used to try to solve the problem in parametric snakes is the Generalized Gradient Vector Flow (GGVF) [13] [14]. Formally, GGVF is defined as a vector field $\mathbf{v}(x, y) = (u(x, y), v(x, y))$ solution of the following partial differential equation:

$$\mathbf{v}_t = g(|\nabla f|) \nabla^2 \mathbf{v} - h(|\nabla f|) (\mathbf{v} - \nabla f) \quad (5)$$

The information from the contours is propagated smoothly where f contains no data, while near the edges \mathbf{v} is desired to be as similar as possible to ∇f . Function $g(|\nabla f|)$ is chosen as complementary to $h(\cdot)$ and governs the trade-off between both terms. Xu et al.[14] use $g(|\nabla f|) = e^{-(|\nabla f|/K)}$ and $h(|\nabla f|) = 1 - g(|\nabla f|)$ to deal with

narrow concavities and some speckle noise when deforming. After the computation of $\mathbf{v}(x, y)$, the external force $-\nabla E_e$ of the snake is replaced by $\mathbf{v}(x, y)$ in (4).

2.3.2. Statistical Snakes

The contours of the likelihood map represent an approximation of the textured region boundaries, and therefore the boundaries of the plaque region. This fact allows us to define explicitly a potential map for the snake to deform allowing us to analyze it and modify it to improve the snake convergence. In particular, we take into account that physics-based as well suffer from a convergence lack to concave boundaries. In order to overcome this drawback, we use the generalized gradient vector flow approach, but applying it on the likelihood map instead of using it over an heuristic created potential field. Note that this process is similar to a regularization procedure performed on the likelihood map.

$$E(\mathbf{v}) = \mu g(|\nabla L|)|\nabla \mathbf{v}|^2 + h(|\nabla L|) \cdot (\mathbf{v} - \nabla L)^2 \quad (6)$$

where $g(|\nabla L|) = e^{-(|\nabla L|/K)}$ and $h(|\nabla L|) = 1 - g(|\nabla L|)$, L is the likelihood map, K and μ are constants. The equilibrium solution to this equation (6) will give a vector field \mathbf{v} to replace the image force of the snake (4). By this formulation we achieve that the vector field \mathbf{v} approximates to the gradient of the contour map in the location of the strong contours of the likelihood map, and smooth otherwise. Moreover, this allows to the snake to surpass weak likelihood contours.

3. EXPERIMENTAL RESULTS

The first step before texture analysis is a polar to cartesian conversion of the image data. This is done to remove the influence of the polar coordinate system over the texture feature extractors, which could not be invariant to rotation. As a consequence of this fact the image contour we are looking for is not closed, it is just a boundary, so we use an open parametric snake deforming from the upper row of the image.

Figure 1 shows a segmentation of an IVUS. Fig. 1.(a) shows the original IVUS image. In fig. 1.(b) the IVUS image is transformed to cartesian coordinates for better performance of the texture descriptors. Figures 1.(c) shows the likelihood map; and fig. 1.(d) shows the contours of the likelihood map; in fig.1.(e) the vector field generated can be observed, note that artifacts appearing are surpassed by the regularization procedure leading to a smooth vector field fig.1.(f) illustrates the final segmentation.

Figure 2 shows an example of deformation of a snake on an IVUS image. We have chosen this image because some artifacts can be seen on in. Fig 2.(a) shows the initial iterations of the snake. Fig.2.(b) illustrates the snake while iterating, note that the artifact effect can be seen in the location of the guide echo. Fig.2.(c) shows the vector

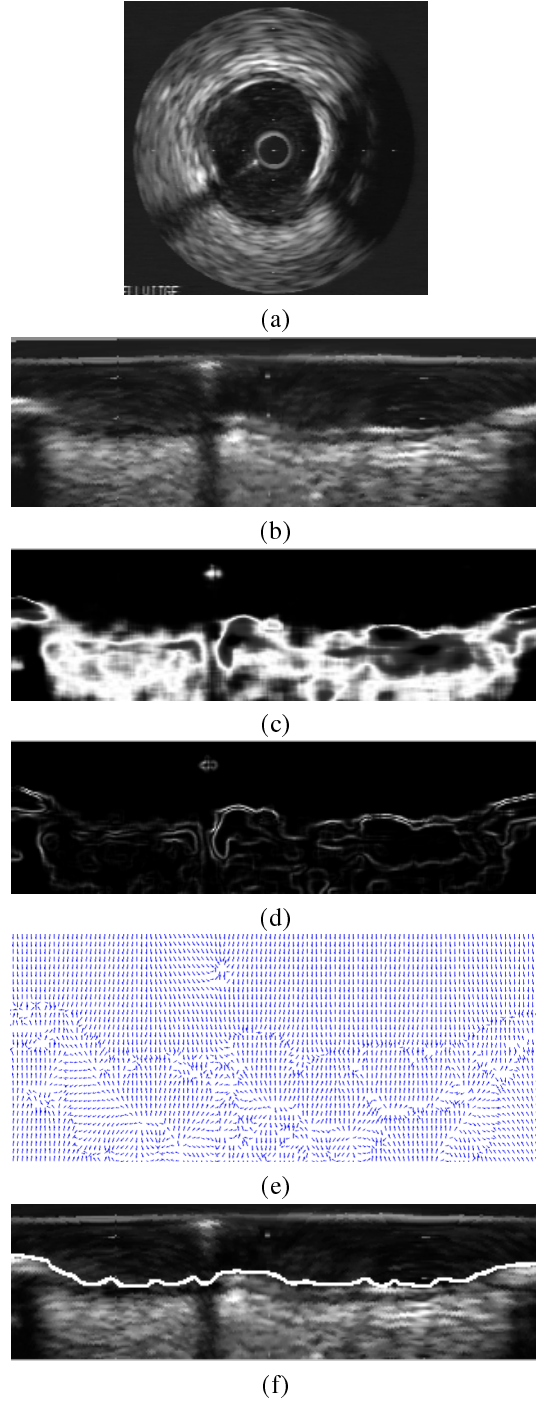


Figure 1. Segmentation of IVUS.(a) Original IVUS image, (b) Original IVUS image in cartesian coordinates, (c) likelihood map (d) contours of the likelihood map (e) vector field generated (f) Location of the lumen-plaque border using the proposed method.

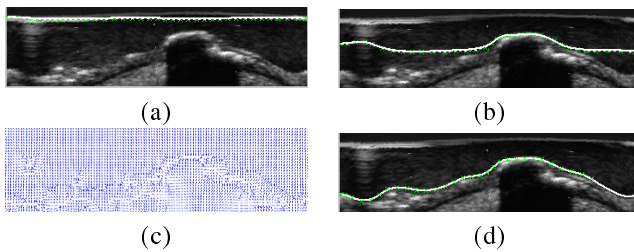


Figure 2. Snake deformation process. (a) Original IVUS image with the snake deforming on its initial iterations, (b) Snake deforming, (c) Vector field for the deformation (d) Deformation complete.

field computed and how the artifacts are surpassed by the regularization procedure. Fig.2.(d) shows the final result of exact adaptation to the lumen boundary.

4. CONCLUSIONS AND FUTURE WORK

We have proposed an automatic segmentation method for lumen detection based on textures and statistic snakes. This method has two main advantages, non-critical initialization issues, as well as, it minimizes the effect of artifacts in the segmentation.

Our future lines consist on extending the method to other domains and application of the method in a geodesic snakes framework for unsupervised tissue characterization.

5. BIBLIOGRAFY

- [1] T. Hofmann, J. Puzicha, and J.M. Buhmann., "Unsupervised texture segmentation in a deterministic annealing framework," *IEEE Transactions on Pattern Analysis and Machine Intelligence*, vol. 20, no. 8, pp. 803–818, 1998.
- [2] J. Malik and P. Perona, "A computational model of texture segmentation.," *In IEEE Conference on Computer Vision and Pattern Recognition*, pp. 326–332, 1989.
- [3] M. Sonka, X. Zhang, and M. Siebes et al, "Segmentation of intravascular ultrasound images: A knowledge based approach," *IEEE Trans. on Medical Imaging*, vol. 14, pp. 719–732, 1995.
- [4] X. Zhang, C.R. McKay, and M. Sonka, "Tissue characterization in intravascular ultrasound images," *IEEE Trans. on Medical Imaging*, vol. 17, pp. 889–899, 1998.
- [5] C. von Birgelen, A. van der Lugt, and A.Ñicosia et al., "Computerized assessment of coronary lumen and atherosclerotic plaque dimensions in three-dimensional intravascular ultrasound correlated with histomorphometry," *Amer. J. Cardiol.*, vol. 78, pp. 1202–1209, 1996.
- [6] K.J. Dixon, D.G. Vince, R.M. Cothren, and J.F. Cornhill, "Characterization of coronary plaque in intravascular ultrasound using histological correlation," *Proceed. 19th Int. Conf. IEEE/EMBS*, vol. 2, 1997.
- [7] J.D. Klingensmith, R. Shekhar, and D.G. Vince, "Evaluation of three-dimensional segmentation algorithms for identification of luminal and medial-adventitial borders in intravascular ultrasound images," *IEEE Trans. on Medical Imaging*, vol. 19, no. 10, pp. 996–1011, 2000.
- [8] R. Haralick, K. Shanmugam, and I. Dinstein, "Textural features for image classification," *IEEE Trans. System, Man, Cybernetics*, vol. 3, pp. 610–621, 1973.
- [9] P.P. Ohanian and R.C. Dubes, "Performance evaluation for four classes of textural features.," *Pattern Recognition*, vol. 25, no. 8, pp. 819–833, 1992.
- [10] Trygve Randen and John H. Husoy, "Filtering for texture classification: A comparative study.," *Pattern Recognition*, vol. 21, no. 4, pp. 291–310, 1999.
- [11] Richard O. Duda, Peter E. Hart, and David G. Stork, *Pattern Classification*, Wiley-Interscience, 2001, 2nd Ed.
- [12] M. Kass, A. Witkin, and D. Terzopoulos., "Snakes, active contour models.," *Int. J. Computer Vision*, vol. 1, no. 4, pp. 321–331, 1987.
- [13] C. Xu and J. L. Prince., "Gradient vector flow: A new external force for snakes.," *IEEE Proc. Conf. on Comp. Vis. Patt. Recog. (CVPR'97)*, pp. 66–71, 1997.
- [14] C. Xu and J. L. Prince., "Generalized gradient vector flow external forces for active contours.," *Signal Processing*, vol. 71, pp. 131–139, 1998.